

ARMY RESEARCH LABORATORY



## Small Scale Burner Review

by Ivan C. Lee

ARL-TR-4881

July 2009

## **NOTICES**

### **Disclaimers**

The findings in this report are not to be construed as an official Department of the Army position unless so designated by other authorized documents.

Citation of manufacturer's or trade names does not constitute an official endorsement or approval of the use thereof.

Destroy this report when it is no longer needed. Do not return it to the originator.

# **Army Research Laboratory**

Adelphi, MD 20783-1197

---

**ARL-TR-4881**

**July 2009**

---

## **Small Scale Burner Review**

**Ivan C. Lee**  
**Sensors and Electron Devices Directorate, ARL**

---

**Approved for public release; distribution unlimited**

---

<b>REPORT DOCUMENTATION PAGE</b>				<b>Form Approved OMB No. 0704-0188</b>
<p>Public reporting burden for this collection of information is estimated to average 1 hour per response, including the time for reviewing instructions, searching existing data sources, gathering and maintaining the data needed, and completing and reviewing the collection information. Send comments regarding this burden estimate or any other aspect of this collection of information, including suggestions for reducing the burden, to Department of Defense, Washington Headquarters Services, Directorate for Information Operations and Reports (0704-0188), 1215 Jefferson Davis Highway, Suite 1204, Arlington, VA 22202-4302. Respondents should be aware that notwithstanding any other provision of law, no person shall be subject to any penalty for failing to comply with a collection of information if it does not display a currently valid OMB control number.</p> <p><b>PLEASE DO NOT RETURN YOUR FORM TO THE ABOVE ADDRESS.</b></p>				
<b>1. REPORT DATE (DD-MM-YYYY)</b> July 2009	<b>2. REPORT TYPE</b> Final	<b>3. DATES COVERED (From - To)</b>		
<b>4. TITLE AND SUBTITLE</b> Small Scale Burner Review		<b>5a. CONTRACT NUMBER</b>		
		<b>5b. GRANT NUMBER</b>		
		<b>5c. PROGRAM ELEMENT NUMBER</b>		
<b>6. AUTHOR(S)</b> Ivan C. Lee		<b>5d. PROJECT NUMBER</b>		
		<b>5e. TASK NUMBER</b>		
		<b>5f. WORK UNIT NUMBER</b>		
<b>7. PERFORMING ORGANIZATION NAME(S) AND ADDRESS(ES)</b> U.S. Army Research Laboratory Attn: RDRL-SED-P 2800 Powder Mill Road Adelphi, MD 20783-1197		<b>8. PERFORMING ORGANIZATION REPORT NUMBER</b> ARL-TR-4881		
<b>9. SPONSORING/MONITORING AGENCY NAME(S) AND ADDRESS(ES)</b>		<b>10. SPONSOR/MONITOR'S ACRONYM(S)</b>		
		<b>11. SPONSOR/MONITOR'S REPORT NUMBER(S)</b>		
<b>12. DISTRIBUTION/AVAILABILITY STATEMENT</b> Approved for public release; distribution unlimited.				
<b>13. SUPPLEMENTARY NOTES</b>				
<b>14. ABSTRACT</b> Microscale combustion differs from the mesoscale or large-scale combustion, in general. As the size of the combustor decreases, surface-to-volume ratio (S/V) increases. Surface effects (interfacial phenomena) and time-scaling become more important. Heat recirculation, combustion in porous media, and catalytic combustion are employed to achieve combustion in microscale. The microscale combustion devices can be integrated with thermoelectric and thermophotovoltaic devices for power and energy applications. Recent advances in microscale combustion are summarized in this report.				
<b>15. SUBJECT TERMS</b> Microcombustion, burner, small scale, micropower, power and energy				
<b>16. SECURITY CLASSIFICATION OF:</b>		<b>17. LIMITATION OF ABSTRACT</b> UU	<b>18. NUMBER OF PAGES</b> 28	<b>19a. NAME OF RESPONSIBLE PERSON</b> Ivan C. Lee
<b>a. REPORT</b> Unclassified	<b>b. ABSTRACT</b> Unclassified	<b>c. THIS PAGE</b> Unclassified		<b>19b. TELEPHONE NUMBER (Include area code)</b> (301) 394-0292

---

## Contents

---

<b>List of Figures</b>	<b>iv</b>
<b>List of Tables</b>	<b>iv</b>
<b>Acknowledgments</b>	<b>v</b>
<b>1. Introduction</b>	<b>1</b>
<b>2. Characteristics and Limitations of Microscale Combustion</b>	<b>1</b>
2.1 Surface Effects (Interfacial Phenomena).....	2
2.2 Time Scaling Effects .....	3
2.3 Flame Ignition, Flame Stability, and Extinction Characteristics in Microchannel .....	3
<b>3. Approaches to Achieve Combustion in Microscale</b>	<b>4</b>
3.1 Heat Recirculation in Microchannels and Swiss Roll Combustors.....	4
3.1.1 Structural Conduction.....	4
3.1.2 Counter Current Recirculation .....	5
3.2 Combustion in Inert Porous Media .....	6
3.3 Catalytic Combustion .....	7
<b>4. Power Systems Integrated with Microcombustors</b>	<b>8</b>
4.1 Thermoelectric (TE).....	8
4.2 Thermophotovoltaic (TPV) .....	10
<b>5. Fuel Issues</b>	<b>11</b>
<b>6. Final Remarks and Recommendations</b>	<b>12</b>
<b>7. References</b>	<b>14</b>
<b>List of Symbols, Abbreviations, and Acronyms</b>	<b>18</b>
<b>Distribution List</b>	<b>19</b>

---

## **List of Figures**

---

Figure 1. Combustor geometry for combustors with (A) structural conduction recirculation and (B) counter-current recirculation.....	5
Figure 2. A microcombustor by Cohen, Ronney, and others (10).....	8
Figure 3. Combustor with backward facing steps.....	11

---

## **List of Tables**

---

Table 1. Selected properties of hydrocarbon fuels (1).....	12
--	----

---

## **Acknowledgments**

---

The author would like to acknowledge Dr. Brian Morgan for reviewing the manuscript and for his comments on thermoelectric devices.

INTENTIONALLY LEFT BLANK.

---

## 1. Introduction

---

Combustion is a study of transforming energy stored in chemical bonds into heat that can be used in various ways (1). This study integrates concepts of chemical kinetics, transport phenomena, and reaction engineering. However, there are no universal definitions of microscale and mesoscale for small scale combustion. The characteristics of microscale combustion have been summarized previously (2). Marbach and Agrawal (3) define microscale as a combustor diameter that is smaller than the quenching diameter of the given fuel. Alternatively, this field can be defined by the level of power output. For example, Fernandez-Pello defines micropower generation as milliwatts to watts level (2). Here we review burner efforts in small scale as defined by dimensions (3) and power output (2), since power density ( $\text{W}/\text{m}^3$ ) is very important to military applications.

Over the past decade, there were tremendous efforts to advance the field of microscale combustion. The main driving force behind these efforts is the much larger energy density of liquid hydrocarbon fuels when compared with batteries. Fernandez-Pello reviewed this subject in 2002 (2), when the field was still in the feasibility stage. Since then, several works have demonstrated the combustion in microscale (4). In addition, some novel approaches have been proposed to understand the fundamental principles of microscale combustion and to circumvent the limitations of microscale combustion. More recently, some research groups have started to build devices that use the microscale combustors or microburners in various applications. As examples, microcomputers or microburners have been integrated with thermoelectric (5–10) and thermophotovoltaic (11, 12) for power and energy applications. Other microcombustion applications include micropropulsion (13, 14), calorimetry (15), and carbon-isotopic analysis in biogeography (16, 17).

The objectives of this report are to first briefly review the characteristics or limitations of fuel combustion in microscale and then to summarize the recent approaches to circumvent these limitations. Next, we highlight some applications of microcombustor for power and energy, including thermoelectric and thermophotovoltaic. At the end of this review we make some recommendations on further research to advance this field. Moreover, the focus is on efforts being reported after Fernandez-Pello's review. Studies on micro heat engines are beyond the scope of this report.

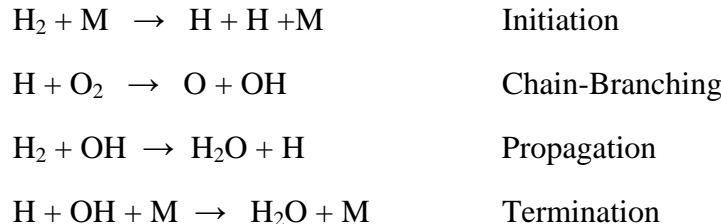
---

## 2. Characteristics and Limitations of Microscale Combustion

---

Typical mechanisms of hydrocarbon combustion involve initiation, propagation, chain-branching, and termination reactions with free radicals as intermediates. Once the combustion is

initiated, chain reactions produce free radicals in the propagation or chain-branching reaction. The free radicals recombine in the termination reactions. For example, H<sub>2</sub>-O<sub>2</sub> combustion consists of as many as 40 reactions and 8 species: H<sub>2</sub>, O<sub>2</sub>, H<sub>2</sub>O, OH, O, H, HO<sub>2</sub> and H<sub>2</sub>O<sub>2</sub> (1). Some of the elementary reactions are



## 2.1 Surface Effects (Interfacial Phenomena)

Microscale combustion differs from the mesoscale, or large-scale, combustion, in general. As the size decreases, surface-to-volume ratio (S/V) increases. Surface effects (interfacial phenomena) (4) and time scaling (4, 18) become more important, and flame quenching (thermal quenching and radical quenching) becomes a problem (4). The consequence is incomplete combustion of hydrocarbon fuels.

In thermal quenching, flame extinction occurs when the heat of combustion cannot compensate the heat loss to the surrounding environment through the wall. The wall acts as an enthalpy sink, and eventually flame extinction occurs. In addition to the heat loss type extinction mechanism, blowout was the second thermal quenching mechanism (19, 20). Blowout occurs when a flame gets swept out of the reactor at low residence time (i.e., high flow rates).

In radical quenching, the free radicals were destroyed to form stable products by undergoing termination reactions at the reactor wall. These wall reactions prevent the buildup of free radicals that would lead to explosions. However, the combustion is terminated if all the radicals recombined to form stable species on the walls of a combustor. When the size of the combustor becomes small, the removal of these radical intermediates is more likely in microscale combustion and disturbs the combustion reactions.

Miesse et al. (4) performed a series of microcombustion experiments to determine quenching distance with various wall materials (quartz, stainless steel, copper, yttria-stabilized zirconia (YSZ), and alumina) at different inside wall temperatures. They concluded that thermal quenching dominates at low temperature (500 K), whereas the radical quenching plays a dominant role at higher temperature (1000 K).

Kim et al. (21) investigated relative significance of heat loss (thermal quenching) and removal of active radicals at the wall (radical quenching) in stoichiometric combustion of a methane-air mixture. They measured quenching distance with virgin and annealed plates of stainless steel, alumina, and quartz at wall temperature from 100–800 °C. Their experimental results indicated that these two quenching phenomena were temperature-dependent. At low temperatures,

quenching distances are independent of the surface characteristics such as oxygen vacancy, grain boundary, or impurities. At high temperatures, surface characteristics strongly affect the quenching distance. These results suggest that radical quenching plays a significant role in the quenching process at high temperatures. Since the typical adiabatic flame temperature of hydrocarbon is over 2200 K, one would expect that minimizing radical quenching is very important for sustaining gas phase microcombustion.

## 2.2 Time Scaling Effects

Time scaling effects also play a critical role in microscale combustion. Theoretically, stable combustion can be achieved when reactant residence time is larger than chemical reaction time and diffusion time (4, 18). Otherwise, incomplete combustion occurs. As a result, lower combustion efficiency will lead to insufficient heat generation to achieve sustained combustion.

At a given fluid (fuel and air) velocity, the reactant residence time decreases with the size of combustor. The conversion (chemical reaction time) is a challenge to maintain stable combustion in microscale. This fundamental time constraint can be quantified in terms of the Damkohler number, which is the ratio of gas residence time to the characteristic chemical reaction time. The Damkohler number must be greater than unity to ensure complete combustion. Superadiabatic combustion has been proposed to increase the Damkohler number and to enhance heat transfer (12). It is noted that superadiabatic combustion offers higher burning rates, increased flame stability, and prolonged residence time because of combined exceptional effects of conduction, radiation, and surface convection. Superadiabatic combustion refers to the strong overheating of the reaction zone, where the temperature far exceeds the thermodynamic combustion temperature (22).

In parallel to this, Reynolds number ( $Re$ ) scales as  $Re \sim L$ , where  $L$  is the characteristic length of the combustor.  $Re$ , therefore, decreases when the combustor becomes smaller.  $Re$  in a microscale combustor is usually much smaller than 2000, at which only laminar flow is possible. Without turbulent mixing, the fuel-air mixing for non-premixed streams would rely on molecular diffusion.

## 2.3 Flame Ignition, Flame Stability, and Extinction Characteristics in Microchannel

Maruta et al. (23) performed experimental studies to investigate the characteristics of microscale combustion in a microchannel heated by an external source. Oscillatory combustion was observed for low velocities of the flow. This can be explained by repetitive extinction and ignition due to the stable-to-unstable transition of the flame.

Miesse et al. (24) studied the microcombustion of methane and observed a sequence of isolated reaction zone structures (flame cells) along the gas flow direction in the microchannel. They summarized the flame stability observation in a flame structure regime map for various initial mixture strength ( $0.29 < \text{equivalent ratio} < 3.5$ ) and total gas flow rate ( $34 \leq Re \leq 82$ ). Prakash et al. (25) modified the previous microcombustor by Miesse et al. (24) such that

chemiluminescence imaging and acoustic emissions can be used to characterize the ignition to transient dynamics and, finally, to formation of a stable edge-like flame and distinct cellular structures. They concluded that the flame cell structure was initially dominated by a hydrodynamic instability, which then transitioned to a steady-state flame cell structure. This stabilization was introduced by a strong coupling between the thermal and fluid fields (25).

In literature, models (26, 27) were developed to explain the experimental observations (28) of flame stabilization, non-linear flame oscillations, and flames with repetitive extinction and ignition. In one study, Minaev et al. (27) proposed a one-dimensional nonlinear evolutionary equation of the flame front model, which took into account the inertial effects such as flame front acceleration and rate of flame temperature variation. These inertial effects were found to be important to describe oscillatory modes of flame propagation.

Kessler and Short (26) described an unsteady ignition sequence in a simple two-dimensional model of a single-pass conductive microburner. Their model predicted the unsteady microcombustion modes, as seen in previous experimental studies (25, 28), in which a reaction wave was driven rapidly down the channel towards the inlet via a sequence of oscillatory ignition and quenching transient extinction and repetitive ignition. This model (26) also showed how the initial axial wall temperature gradient was found to be central to determining combustion evolution to a variety of sustained combustion modes.

---

### **3. Approaches to Achieve Combustion in Microscale**

---

#### **3.1 Heat Recirculation in Microchannels and Swiss Roll Combustors**

Heat recirculation is one possible solution to redistributing thermal energy within a microcombustor and minimizing the heat losses to the outside environment. A simple model of a heat recirculation-type burner is combustion in a narrow channel surrounded by a high temperature wall (19, 18, 29, 30–32) or recirculation of hot exhaust gas (33–35) (figure 1). Another example of heat recirculation is the combustion in porous media (3, 36–38).

##### **3.1.1 Structural Conduction**

Redistribution or recirculation of heat can be accomplished by structural conduction, in which heat is conducted from a hot combustor wall downstream to a colder portion upstream. Leach et al. (32) presented a one-dimensional model to investigate the effect of structural conduction and heat loss on hydrogen-air combustion in microchannels. Their results indicated that increasing conductance of the structure, by either increasing thermal conductivity or the structure thickness, would increase the amplitude of reaction zone broadening. In other studies,

Hua et al. (18, 29) also investigated the microcombustion mechanism of a hydrogen-air mixture with numerical simulations. Although lower wall heat conductivity can reduce the heat loss, it may also cause a hot spot on the wall near the flame and high temperature gradient in the wall.

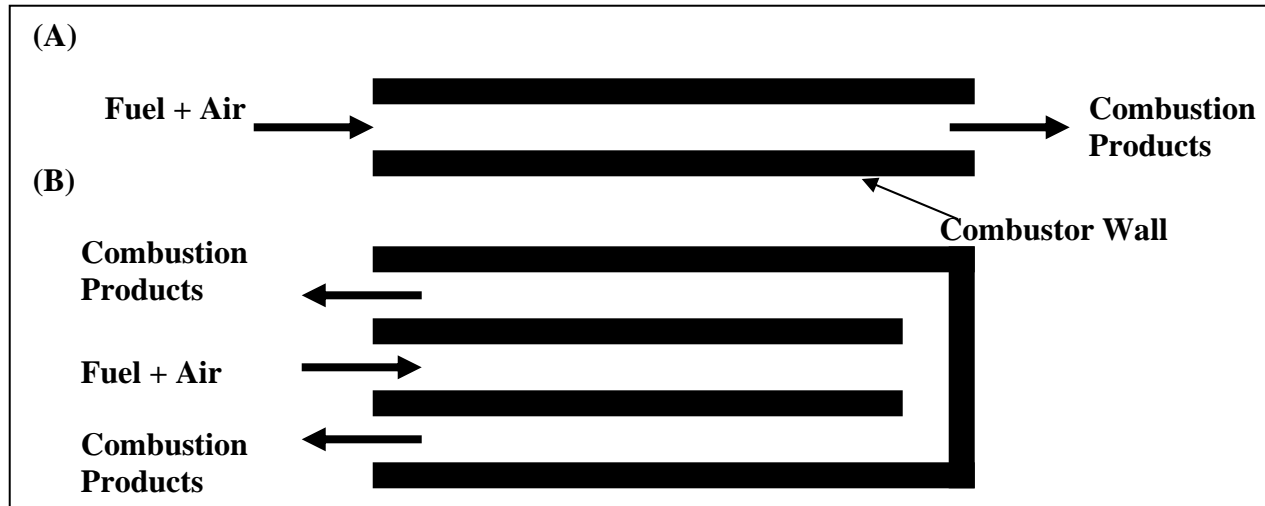


Figure 1. Combustor geometry for combustors with (A) structural conduction recirculation and (B) counter-current recirculation.

Kaisare and Vlachos (19) presented a comprehensive study about the effects of reactor dimensions and operating conditions on thermal quenching. They have studied the roles of heat recirculation and heat loss on the flame extinction and blowout in microscale (<1 mm) combustion. For instance, stabilization of flame can be achieved by the heat recirculated upstream through the reactor solid structure. Moreover, extinction has a stronger dependence on heat loss to surroundings than on blowout. In addition, Norton and Vlachos (30, 31) also found that wall thermal conductivity was vital in determining the flame stability of propane/air and methane/air combustion in microscale. Their two-dimensional elliptic computational fluid dynamics (CFD) model showed that the walls transferred heat upstream for ignition of the cold incoming fuel-air mixtures but were also responsible for the external heat loss.

### 3.1.2 Counter Current Recirculation

In addition to structural conduction by wall, heat loss to the surrounding can be minimized by counter-current recirculation as similar to the geometry in figure 1 (B). Recently, Federici and Vlachos (35) performed additional CFD modeling to study flame stability of propane-air combustion in microchannels with hot combustion gas product flowing countercurrent to preheat the reactants. The resultant heat recirculation through hot exhaust gas would increase flame stability in the limit of a low-conductivity wall or high flow velocity (i.e., blowout mode of flame stability).

Early work on the Swiss-roll combustor by Weinberg, Ronney, Marruta, and others was reviewed by Fernandez-Pello in 2002 (2). Recently, Kim et al. (33) investigated the channel width of the combustors, which was smaller than the quenching distance of propane flame. Their results implied that mean temperature and the flammability limits of the combustors were governed by both the radiation heat loss and the total chemical energy introduced to the combustors. It was also shown that thermal efficiency increased as the combustor became smaller. Although  $\text{NO}_x$  emission decreased with combustor size, carbon monoxide (CO) emission became an issue. They found that addition of a catalyst at the exhaust would eliminate the CO emission.

Ronney (34) developed a first-principles model of counter-current heat recirculation combustors. Ronney compared the counter-current heat recirculation configuration with conductive tube configuration (i.e., single pass microchannel). The performance of structural conduction through the combustor wall was demonstrated to be inferior to that of the counter-current configuration. In heat recirculation via structural conduction (conductive tube configuration), much higher fuel concentration was necessary to sustain combustion in same mass flux (or same Re).

### 3.2 Combustion in Inert Porous Media

The principle behind combustion in porous media is the concept of excess enthalpy and heat transfer mechanism (39). In this mechanism the flame produced from the combustion zone convectively heats the solid porous medium, which transfers the heat upstream to preheat the inert mixture through conduction and radiation. In order to stabilize the combustion process, the effective flame speed is equal to the incoming velocity (41). This can be achieved by a balance among heat recirculation, heat release, and heat loss.

Barra and Ellzey (38) developed a numerical model to quantify heat recirculation and to analyze the dominant heat transfer processes responsible for heat recirculation. They demonstrated that heat recirculation efficiency decreased with increasing equivalence ratio. In addition, the dominant role of heat recirculation depends on equivalence ratio and flame speed ratio, as radiation became the dominant mode with increasing equivalence ratio and flame speed.

Marbach and Agrawal (36, 3, 37) investigated methane combustion experimentally and computationally using a heat recirculation combustor with porous inert media made of silicon carbide-coated carbon foam. Results showed that the reactant was preheated to 600 K using the thermal energy from the reaction zone, which allowed very lean combustion. In other words, combustion in porous inert media is an effective method to extend the blow-off limit in lean premixed combustion. The researchers found that the maximum product gas temperature was higher than the adiabatic flame temperature of the reactants at inlet conditions. Their design also achieved effective heat recirculation so that heat loss to the surrounding environment was minimized. They suggested that the heat recirculation could be used to pre-vaporize liquid fuels. In a later work, Newburn and Agrawal (40) designed and tested a heat recirculation combustor of

kerosene with a porous media (stainless steel beads) filled annular preheating section. Heat transfer and combustion performance were evaluated experimentally at various equivalence ratios, heat release rates, and inlet air temperature. Low emission of CO was observed.

### 3.3 Catalytic Combustion

An alternative to homogenous combustion, as described above, is heterogeneous catalytic combustion. Firstly, the characteristic time scale for combustion can be shortened in the presence of a catalytic surface, as Damkohler number increases in their presence. Secondly, catalytic combustion proceeds with lower temperatures than homogeneous combustion. Typical adiabatic flame temperatures of hydrocarbons in homogenous combustion are larger than 2200 K, and the typical wall temperature for the homogeneous microcombustor is still around 1000 K. At these high temperatures, construction materials of the microcombustor system may crack or melt and the choice of materials become limited. As we will discuss later, the current state-of-the-art thermoelectric materials will break at such a high temperature gradient (room temperature as cold side). Studies in catalytic combustion were initiated to circumvent the problem of material failure.

Since methane is the simplest hydrocarbon and the only hydrocarbon with a reliable, detailed surface reaction mechanism, most of the computational studies employ methane as the model fuel (20, 42). Li and Im (42) performed numerical simulations of an on-chip microcombustor in stagnation-point flow geometry with a catalytic surface to elucidate the physical and chemical characteristics in catalytic combustion. Their results showed bifurcation behavior, which is gas-phase reaction dominating at high temperatures and surface reaction dominating at lower temperatures. By comparing the extinction strain rates for methane-air combustion with and without surface reaction, they concluded that surface reaction can substantially extend the range of stable combustion. They have also confirmed that the characteristic time scale for the surface reaction is shorter than that for the gas-phase reactions under their reaction conditions.

Maruta and others (20) used computational methods to examine the extinction limits for self-sustaining catalytic combustion of methane-air mixtures in microscale channels. The geometry of the microcombustor was chosen so that axial heat conduction and gas-phase reactions can be neglected. Instead of wall temperatures that were artificially imposed, this study determined the actual temperature profiles in which the microcombustor was self-sustained with heat release due to surface reaction and heat loss to the surrounding environment. They found that the equivalence ratio at the extinction limit monotonically decreased with increasing  $Re$  under adiabatic boundary conditions. When heat loss exists, the extinction curve exhibited U-shaped dual limit behavior (figure 2). They concluded that extinction limits were caused by heat loss through the wall, and the latter was a blow-off extinction due to insufficient residence time compared to the chemical time-scale. These two limits were characterized by platinum (Pt) and oxygen (O) surface coverage. Heat-loss extinction occurred when surface coverage of Pt(s) is small and surface coverage of O(s) is large. In addition, their results also suggested that near-

stoichiometric mixtures and exhaust gas recirculation, rather than lean mixtures, are preferable for minimizing flame temperatures in catalytic microcombustors. These findings were also confirmed with another study with propane fuel by one of the co-workers (43).

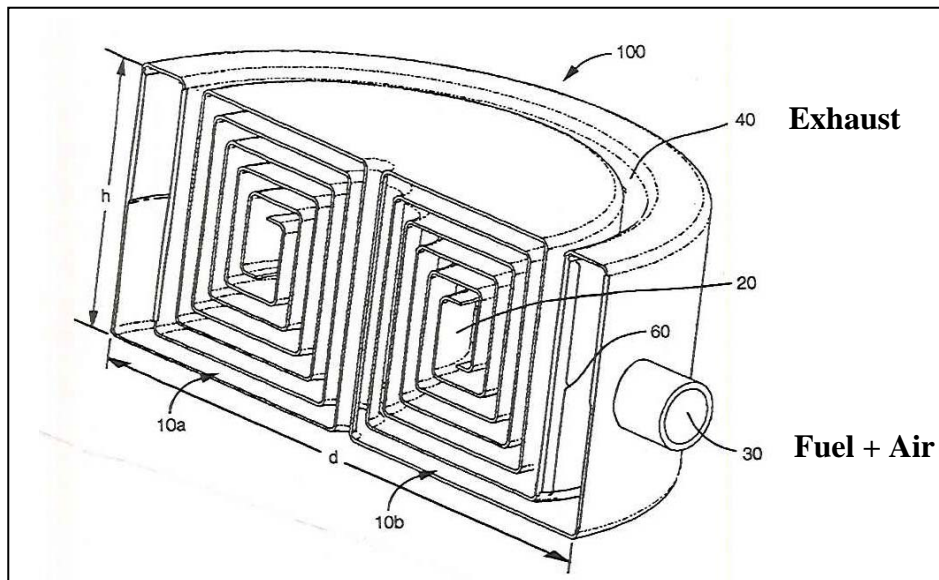


Figure 2. A microcombustor by Cohen, Ronney, and others (10).

Ahn et al. (43) conducted experiments to examine the extinction limits and temperature characteristics of heat-recirculating Swiss-roll combustors with catalytic and non-catalytic (gas-phase) combustion of propane over a large range of  $Re$ . The presence of a catalyst lowered the apparent activation energy of combustion. Catalytic combustion could be sustained in the Swiss-roll burner at minimum  $Re = 1$  and at an extremely low temperature (350 K).

Gomez group investigated liquid fuel catalytic microcombustors using electrospray devices as fuel atomizers (44, 45). Depending on the flow rate of a single JP-8 electrospray in the cone-jet regime, the droplet diameter was between 10 to 40 microns. The multiplexed atomizer provided a spray of fine liquid fuel droplets for good fuel and air mixing. This fuel-air mixture was fully combusted to give CO/carbon dioxide ( $CO_2$ ) ratio of less than 1% (45).

---

## 4. Power Systems Integrated with Microcombustors

---

### 4.1 Thermoelectric (TE)

In a typical TE power system (5), the major components include a catalytic microscale combustor, thermal spreaders, a TE device and a heat sink. The heat generated in the microcombustor (hot side temperature  $T_2$ ) is conducted through the spreaders to the TE device, which is connected to a heat sink (cold side temperature  $T_1$ ). The TE device operates according to the Seebeck effect, where two materials (one is p-type and another one is n-type) with two

different Seebeck coefficients are connecting to support a thermal gradient (T2-T1). A binary bismuth telluride compound, such as  $\text{Bi}_2\text{Te}_3$ , and ternary compound, such as  $\text{Bi}_{2-x}\text{Sb}_x\text{Te}_3$ , are common n-type and p-type TE materials, respectively.

Although the power generated from TE devices is proportional to the square of the thermal gradient (T2-T1), typical commercial TE devices have a practical limit of 300 °C because of the melting and degradation of materials in the devices, as well as migration of dopants in the semiconductor components of the devices (5). Venkatasubramanian (46) reviewed some state-of-the-art TE materials such as quantum-dot superlattices, which are under development for applications in 300–500 °C ranges.

Cohen, Ronney, and others (10) published a patent on a microcombustion-based thermoelectric generator. As shown in figure 2, in their design (a variation of Swiss-roll type combustor) the reactant channel and exhaust channels were coiled around each other in a spiral configuration so that heat loss was reduced. Some T-shaped or L-shaped fins were parts of the thermoelectric active wall. Some fins were extended in the reactant channel, while others were extended in the exhaust channel. These fins were designed to act as a diffusion barrier between the n-type and p-type TE materials and to increase the thermal gradient.

Minaev and Fursenko (7) developed a mathematic model to estimate the efficiency of an integrated system with a homogeneous microcombustion channel for pre-mixed gas and TE devices for energy conversion. They found that the highest efficiency can usually be reached near the flammability limits. In other words, the issues of flammability limits and flame stability are directly related to the efficiency of the integrated device.

Yoshida et al. (9) have demonstrated that an integrated TE system can operate at total efficiency of 2.8% by installing two TE modules on both sides of a microcombustor. Microcombustion of butane was demonstrated with 100% combustion efficiency and uniform temperature distribution. However, resistive heating is required to ignite the fuel. In addition, only hydrogen combustion could be sustained when integrated with a TE device. Their integrated TE system was evaluated with hydrogen-air fuel combustion with a Pt catalyst and achieved power generation of 0.184 W at a total efficiency of 2.8%. It was suggested that a higher performance catalyst and an improved system design were needed to use butane in the integrated TE system.

Vlachos et al. (5, 6, 8) performed microcombustion experiments and fabricated an integrated TE system using hydrogen-air, propane-air, and methanol-air fuel mixtures at stoichiometric and fuel-lean conditions with Pt-alumina catalyst inserts in a stainless steel microcombustor. It was found that thermal properties of the microcombustor wall have a substantial effect on microcombustor thermal uniformity (8). They applied thermally conductive metal (copper [Cu]) spreaders to increase axial thermal uniformity along the microcombustor and to transport heat uniformly over the full footprint of the TE device. These studies also investigated the effects of fuel and flow rate on power generation, as well as heat removal from the cold side. Power generation was found to increase with fuel/air flow rate. When the load resistance matched with

the internal resistance of the TE device, optimal power generation was obtained. The group also found that power generation was substantially improved by forced convection to augment heat removal from TE device. For the methanol integrated microcombustion-TE power system, maximum power generated was 0.65 W with maximum thermal efficiency of 1.1% (6).

## 4.2 Thermophotovoltaic (TPV)

In a typical thermophotovoltaic (TPV) power system, there are three major components: microcombustor, TPV infrared optics/emitters, and TPV cells. TPV cells enclose the combustor peripherally such that heat is transferred from the wall of the combustor to the TPV cells by radiation (12). Then this radiative heat is converted to electricity directly. Gallium antimonide (GaSb) and indium gallium arsenide (InGaAs) are common TPV cell materials. Like TE devices, TPV devices do not have any moving parts, so friction loss is not an issue when we scale down these devices to integrate with the microcombustor. In addition, size reduction (increase in S/V ratio) enhances the output of radiation power per unit volume through the outer surface of the microcombustor drastically.

The fundamental principle of a TPV process is that TPV cells convert photons from the radiation spectrum to the photoelectrons if the photons have energies greater than the band gap of the TPV cells. Conversely, the photon with lower energies would become waste and even a destructive heat load to the TPV cells. Therefore, Xue et al. (12) have proposed the use of a selective emitter to reshape the radiation spectrum. They also suggested the use of an optical filter inserted between a blackbody emitter and the TPV cell array to reflect unusable radiation heat back to the combustion wall. Due to the higher order temperature scaling in TPV device, one would expect radiation heat transfer in TPV would be more effective than the TE device when the combustor operates at high temperatures.

Xue et al. (12) have analyzed the energy conversion efficiency of a GaSb micro TPV system incorporating broadband silicon carbide (SiC) and selective emitted materials (cobalt [Co]/nickel [Ni]-doped magnesium oxide [MgO]). Use of a backward-facing step in the microcombustor (figure 3) achieved a uniform wall temperature at 1000 K (47). The backward-facing step enhanced the mixing process of the fuel mixture and prolonged the residence time.

Consequently, the position of the flame can be effectively controlled, and the range of operation was widened. They also fabricated a novel micro TPV power system that can produce measured electric power output ranging from 0.07 W to 0.74 W with the hydrogen-air mixture (12). This prototype used SiC as the material for the microcombustor and emitter, and a hexagonal GaSb TPV cell array. Since the operation temperatures of the TPV cell affect the power output and reverse saturation current, effective cooling would be necessary.

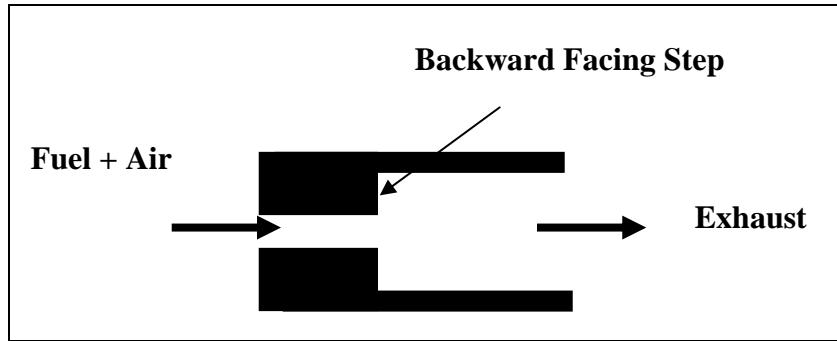


Figure 3. Combustor with backward facing steps.

In a recent study Lee and Kwon (11) investigated a heat-recirculating microemitter (microcombustor) using a propane-air mixture for the micro-TPV system. They applied the heat recirculation concept in a cylindrical microcombustor with an annular-type shield to achieve stable burning in small confinement, maximum heat transfer and uniform wall temperature distribution. As a result, heat generated in the microcombustor was uniformly emitted. Their experimental and computational results show that thermal characteristics along the microcombustor wall were improved with decreasing wall thickness, as well as increasing ratios of the inner radius of the shield to the gap between the shield and microcombustor wall. Based on these results, they proposed a conceptual design for such a system with estimated overall efficiency and output power of 4.3% and 4.2 W, respectively.

---

## 5. Fuel Issues

---

It should be noted that the majority of literature on the microcombustion has been focused on combustion of gaseous hydrocarbons such as methane and propane. In practical military applications, the use of liquid hydrocarbons is more realistic; therefore, we briefly review some of the fuel properties at the end of this report.

As shown in table 1, n-butane and smaller hydrocarbons are gaseous compounds at atmospheric pressure. Butane has a boiling point of  $-0.5^{\circ}\text{C}$ , and it can be liquefied with a small applied pressure. Methane consists of four hydrogen atoms for each carbon (C) atom, and it has the highest heating value among the hydrocarbons. The heating values decrease when the size of hydrocarbon increases.

Table 1. Selected properties of hydrocarbon fuels (1).

Fuel	Formula	Boiling Point, °C	Lower Heating Value, kJ/kg	Adiabatic Flame Temp., K
Methane	CH <sub>4</sub>	-164	50,016	2,226
Ethane	C <sub>2</sub> H <sub>6</sub>	-88.6	47,489	2,259
Propane	C <sub>3</sub> H <sub>8</sub>	-42.1	46,357	2,267
n-Butane	C <sub>4</sub> H <sub>10</sub>	-0.5	45,742	2,270
n-Pentane	C <sub>5</sub> H <sub>12</sub>	36.1	45,355	2,272
Benzene	C <sub>6</sub> H <sub>6</sub>	80.1	40,579	2,342
n-Hexane	C <sub>6</sub> H <sub>14</sub>	69	45,105	2,273
n-Heptane	C <sub>7</sub> H <sub>16</sub>	98.4	44,926	2,274
n-Octane	C <sub>8</sub> H <sub>18</sub>	125.7	44,791	2,275
n-Nonane	C <sub>9</sub> H <sub>20</sub>	150.8	44,686	2,276
n-Decane	C <sub>10</sub> H <sub>22</sub>	174.1	44,602	2,277
n-Undecane	C <sub>11</sub> H <sub>24</sub>	195.9	44,532	2,277
n-Dodecane	C <sub>12</sub> H <sub>26</sub>	216.3	44,467	2,277

Dealing with liquid fuels in microcombustion would require additional research efforts in fuel evaporation or fuel-air mixture. Droplet evaporation of a single hydrocarbon in air is a classic Stefan diffusion tube problem in a spherically symmetric coordinate system (1). Since JP-8 is a mixture of liquid hydrocarbons with different saturated pressures, solving the Stefan problem with multi-components is much more complicated. In literature, there were some previous efforts to atomize liquid fuel to form small fuel droplets prior to combustion (44, 45).

Finally, carbon management and sulfur management are other important issues in JP-8 combustion. These issues were reviewed previously (48). In JP-8 microcombustion, soot formation and fouling on the wall would potentially lower the efficiency of gas-phase combustion. In addition, the sulfur content in JP-8 can be as high as 3000 ppm according to military specifications. As a result, sulfur-tolerant catalysts are needed to avoid sulfur poisoning in catalytic combustion.

## 6. Final Remarks and Recommendations

This report clearly demonstrated that further understanding of chemical kinetics and transport phenomena is critical to advance the field of microcombustion or microburner. Additional works are needed to optimize the combustor geometry while coupling it with oxidation kinetics of heavy hydrocarbons. Catalytic combustion offers some opportunities for lower combustion temperature and shorter reaction time; research in this area, however, is still very limited. Recent works also have suggested that counter-current recirculation of heat, in addition to structural conduction, is a good approach for thermal management.

Most of the microburner efforts were focusing on gaseous fuels such as hydrogen, methane, and propane. Only very limited works were conducted on liquid fuels, which are more practical for military applications. This field is limited by our current understanding on the combustion mechanism of hydrocarbon because we only understand the full mechanism for very small hydrocarbons, such as methane. Therefore, we need to develop full mechanisms with gas-phase and catalytic combustion, as well as to validate these mechanisms with experimental data.

Last but not least, we also need to investigate the means to atomize liquid fuels into small droplets and to understand droplet evaporation or burning for multi-component mixtures because real fuels, such as JP-8 and diesel, are mixtures of liquid hydrocarbon.

---

## 7. References

---

1. Turns, S. R. *An Introduction to Combustion*, McGraw Hill, 2<sup>nd</sup> Edition (2000)
2. Fernandez-Pello, A. C. Micropower Generation Using Combustion: Issues and Approaches. *Proceedings of the Combustion Institute* **2002**, 29, 883.
3. Marbach, T. L.; Agrawal, A. K. Heat-recirculating Combustor Using Porous Inert Media for Mesoscale Applications. *Journal of Propulsion & Power* **2006**, 22, 145.
4. Miesse, C. M.; Masel, R. I.; Jensen, C. D.; Shannon, M. A.; Short, M. Submillimeter-scale Combustion. *AICHE J.* **2004**, 50, 3206.
5. Federici, J. A.; Norton, D. G.; Bruggemann, T.; Voit, K. W.; Wetzel, E. D.; Vlachos, D. G. Catalytic Microcombustors With Integrated Thermoelectric Elements for Portable Power Production. *Journal of Power Sources* **2006**, 161, 1469–1478.
6. Karim, A. M.; Federici, J. A.; Vlachos, D. G. Portable Power Production from Methanol in an Integrated Thermoelectric/Microreactor System. *Journal of Power Sources* **2008**, 179, 113–120.
7. Minaev, S. S.; Fursenko, R. V. Estimates of Efficiency of a Small-size Thermoelectric Channel in Terms of Conversion of Heat Produced by Gas Combustion to Electric Power. *Combustion Explosion & Shock Waves* **2007**, 43, 384–390.
8. Norton, D. G.; Wetzel, E. D.; Vlachos, D. G. Thermal Management in Catalytic Microreactors. *Ind. Eng. Chem. Res.* **2006**, 45, 76.
9. Yoshida, K.; Tanaka, S.; Tomonari, S.; Satoh, D.; Esashi, M. High Energy Density Miniature Thermoelectric Generator Using Catalytic Combustion. *J. Microelectromech. Syst.* **2006**, 15, 195.
10. Cohen, Ai.; Ronney, P.; Frodis, U.; Sitzki, L.; Meiburg, E.; Wussow S. Microcombustion and Combustion-Based Thermoelectric Microgenerator. U.S. Patent 6,613,972 B2, September 2, 2003.
11. Lee, K. H.; Kwon, O. C. Studies on a Heat-recirculating Microemitter for a Micro thermophotovoltaic System. *Combustion & Flame* **2008**, 153, 161.
12. Xue, H.; Yang, W. M.; Chou, S. K.; Shu, C.; Li, Z. W. Microthermophotovoltaics power system for portable mems devices. *Microscale Thermophysical Engineering* **2005**, 9, 85.

13. Chaalane, A.; Rossi, C.; Esteve, D. The Formulation and Testing of New Solid Propellant Mixture (DB plus x%BP) for a New MEMS-based Microthruster. *Sensors and Actuators A-Physical* **2007**, *138*, 161.
14. Son, S. F.; Asay, B. W.; Foley, T. J.; Yetter, R. A.; Wu, M. H.; Risha, G. A. Combustion of nanoscale Al/MoO<sub>3</sub> thermite in microchannels. *Journal of Propulsion and Power* **2007**, *23*, 715.
15. Morgan, A. B.; Galaska M. Microcombustion Calorimetry as a Tool for Screening Flame Retardancy in Epoxy. *Polymers for Advanced Technologies* **2008**, *19*, 530.
16. Eek, K. M.; Sessions, A. L.; Lies, D. P. Carbon-isotopic Analysis of Microbial Cells Sorted by Flow Cytometry. *Geobiology* **2007**, *5*, 85.
17. Nelson, D. M.; Hu, F. S.; Mikucki, J. A.; Tian, J.; Pearson, A. Carbon-isotopic Analysis of Individual Pollen Grains from C-3 and C-4 Grasses Using a Spooling-wire Microcombustion Interface. *Geochimica et Cosmochimica Acta* **2007**, *71*, 4005.
18. Hua, J. S.; Wu, M.; Kumar, K. Numerical Simulation of the Combustion of Hydrogen-air Mixture in Micro-scaled Chambers. Part I: Fundamental Study. *Chemical Engineering Science* **2005**, *60*, 3497.
19. Kaisare, N. S.; Vlachos, D. G. Optimal Reactor Dimensions for Homogeneous Combustion in Small Channels. *Catalysis Today* **2007**, *120*, 96.
20. Maruta, K.; Takeda, K.; Ahn, J.; Borer, K.; Sitzki, L.; Ronney, P. D.; Deutschmann, O. Extinction Limits of Catalytic Combustion in Microchannels. *Proceedings of the Combustion Institute* **2002**, *29*, 957.
21. Kim, K. T.; Dae, H.L.B.; Kwon, S. Effects of Thermal and Chemical Surface-flame Interaction on Flame Quenching. *Combustion & Flame* **2006**, *146*, 19.
22. Aldushin, A. P.; Rumanov, I. E.; Matkowsky, B. J. Maximal Energy Accumulation in a Superadiabatic Filtration Combustion Wave. *Combustion & Flame* **1999**, *118*, 76.
23. Maruta, K.; Parc, J. K.; Oh, K. C.; Fujimori, T.; Minaev, S. S.; Fursenko, R. V. Characteristics of Microscale Combustion in a Narrow Heated Channel. *Combustion Explosion and Shock Waves* **2004**, *40*, 516.
24. Miesse, C.; Masel, R. I.; Short, M.; Shannon, M. A. Experimental Observations of Methane-oxygen Diffusion Flame Structure in a Sub-millimetre Microburner. *Combustion Theory and Modelling* **2005**, *9*, 77.
25. Prakash, S.; Armijo, A. D.; Masel, R. I.; Shannon, M. A. Flame Dynamics and Structure Within Sub-millimeter Combustors. *AICHE J* **2007**, *53*, 1568.

26. Kessler, D. A.; Short, M. Ignition and Transient Dynamics of Sub-limit Premixed Flames in Microchannels. *Combustion Theory and Modelling* **2008**, *12*, 809.
27. Minaev, S.; Maruta, K.; Fursenko, R. Nonlinear Dynamics of Flame in a Narrow Channel with a Temperature Gradient. *Combustion Theory and Modelling* **2007**, *11*, 187.
28. Maruta, K.; Kataoka, T.; Kim, N. I.; Minaev, S.; Fursenko, R. Characteristics of Combustion in a Narrow Channel with a Temperature Gradient. *Proceedings of the Combustion Institute* **2005**, *30*, 2429.
29. Hua, J. S.; Wu, M.; Kumar, K. Numerical Simulation of the Combustion of Hydrogen-air Mixture in Micro-scaled Chambers: Part II: CFD Snalysis for a Micro-combustor. *Chemical Engineering Science* **2005**, *60*, 3507.
30. Norton, D. G.; Vlachos, D. G. A CFD Study of Propane/Air Microflame Stability. *Combustion & Flame*, **2004**, *138*, 97.
31. Norton, D. G.; Vlachos, D. G. Combustion Characteristics and Flame Stability at the Microscale: a CFD Study of Premixed Methane/Air Mixtures. *Chemical Engineering Science* **2003**, *58*, 4871.
32. Leach, T. T.; Cadou, C. P.; Jackson, G. S. Effect of Structural Conduction and Heat Loss on Combustion in Micro-channels. *Combustion Theory and Modelling* **2006**, *10*, 85.
33. Kim, N. I.; Kato, S.; Kataoka, T.; Yokomori, T.; Maruyama. S.; Fujimori, T.; Maruta, K. Flame Stabilization and Emission of Small Swiss-roll Combustors as Heaters. *Combustion and Flame* **2005**, *141*, 229.
34. Ronney, P. D. Analysis of Non-adiabatic Heat-recirculating Combustors. *Combustion and Flame* **2003**, *135*, 421.
35. Federici, J. A.; Vlachos, D. G. A Computational Fluid Dynamics Study of Propane/Air Microflame Stability in a Heat Recirculation Reactor. *Combustion & Flame* **2008**, *153*, 258.
36. Marbach, T. L.; Sadasivuni, V.; Agrawal, A. K. Investigation of a Miniature Combustor Using Porous Media Surface Stabilized Flame. *Combustion Science & Technology* **2007**, *179*, 1901.
37. Marbach, T. L.; Agrawal, A. K. Experimental Study of Surface and Interior Combustion Using Composite Porous Inert Media. *Journal of Engineering for Gas Turbines & Power-Transactions of the ASME* **2005**, *127*, 307.
38. Barra, A. J.; Ellzey, J. L. Heat Recirculation and Heat Transfer in Porous Burners. *Combustion & Flame* **2004**, *137*, 230.
39. Kamal, M. M.; Mohamad, A. A. Combustion in Porous Media. *Proceedings of the Institution of Mechanical Engineers Part A – Journal of Power and Energy* **2006**, *220*, 487.

40. Newburn, E. R.; Agrawal, A. K. Liquid Fuel Combustion Using Heat Recirculation Through Annular Porous Media. *Journal of Engineering for Gas Turbines and Power-Transactions of the ASME* **2007**, *129*, 914.
41. Wood, S.; Harris, A. T. Porous Burners for Lean-burn Applications. *Progress in Energy and Combustion Science* **2008**, *34*, 667.
42. Li, J. J.; Im, H. G. Extinction Characteristics of Catalyst-assisted Combustion in a Stagnation-point Flow Reactor. *Combustion & Flame* **2006**, *145*, 390.
43. Ahn, J. M.; Eastwood, C.; Sitzki, L.; Ronney, P. D. Gas-phase and Catalytic Combustion in Heat-recirculating Burners. *Proceedings of the Combustion Institute* **2006**, *30*, 2463.
44. Kyritsis, D. C.; Coriton, B.; Faure, F.; Roychoudhury, S.; Gomez, A. Optimization of a Catalytic Combustor Using Electrosprayed Liquid Hydrocarbons for Mesoscale Power Generation. *Combustion & Flame* **2004**, *139*, 77.
45. Deng, W. W.; Klemic, J. F.; Li, X. H.; Reed, M. A.; Gomez, A. Liquid Fuel Microcombustor Using Microfabricated Multiplexed Electrospray Sources. *Proceedings of the Combustion Institute* **2007**, *31*, 2239.
46. Venkatasubramanian, R.; Watkins, C.; Caylor, C.; Bulman, G. Microscale Thermoelectric Devices for Energy Harvesting and Thermal Management. *Technical Digest, Power MEMS 2006*, *1*.
47. Yang, UY. M.; Chou, S. K.; Shu, C.; Li, Z. W.; Xue, H. Combustion in Micro-cylindrical Combustors With and Without a Backward Facing Step. *Applied Thermal Engineering* **2007**, *22*, 1777.
48. Lee, I. C.; Chu, D. *Literature Review of Fuel Processing*; ARL-TR-2946; Harry Diamond Laboratory: Adelphi, MD, March 2003.

---

## **List of Symbols, Abbreviations, and Acronyms**

---

C	carbon
CFD	computational fluid dynamics
Co	cobalt
CO	carbon monoxide
CO <sub>2</sub>	carbon dioxide
Cu	copper
GaSb	gallium antimonide
InGaAs	indium gallium arsenide
MgO	doped magnesium oxide
Ni	nickel
O	oxygen
Pt	platinum
Re	Reynolds number
SiC	silicon carbide
S/V	surface-to-volume ratio
TE	thermoelectric
TPV	thermophotovoltaic
YSZ	yttrium-stabilized zirconia

<u>No. of Copies</u>	<u>Organization</u>	<u>No. of Copies</u>	<u>Organization</u>
1 ELECT	ADMNSTR DEFNS TECHL INFO CTR ATTN DTIC OCP 8725 JOHN J KINGMAN RD STE 0944 FT BELVOIR VA 22060-6218	1	COMMANDER US ARMY RDECOM ATTN AMSRD AMR W C MCCORKLE 5400 FOWLER RD REDSTONE ARSENAL AL 35898-5000
1	DARPA ATTN IXO S WELBY 3701 N FAIRFAX DR ARLINGTON VA 22203-1714	1	US GOVERNMENT PRINT OFF DEPOSITORY RECEIVING SECTION ATTN MAIL STOP IDAD J TATE 732 NORTH CAPITOL ST NW WASHINGTON DC 20402
1 CD	OFC OF THE SECY OF DEFNS ATTN ODDRE (R&AT) THE PENTAGON WASHINGTON DC 20301-3080	1	US ARMY RSRCH LAB ATTN RDRL CIM G T LANDFRIED BLDG 4600 ABERDEEN PROVING GROUND MD 21005-5066
1	US ARMY RSRCH DEV AND ENGRG CMND ARMAMENT RSRCH DEV AND ENGRG CTR ARMAMENT ENGRG AND TECHNLGY CTR ATTN AMSRD AAR AEF T J MATT BLDG 305 ABERDEEN PROVING GROUND MD 21005-5001	24	US ARMY RSRCH LAB ATTN IMNE ALC HRR MAIL & RECORDS MGMT ATTN RDRL CIM L TECHL LIB ATTN RDRL CIM P TECHL PUB ATTN RDRL SED P I LEE (20 COPIES) ADELPHI MD 20783-1197
1	PM TIMS, PROFILER (MMS-P) AN/TMQ-52 ATTN B GRIFFIES BUILDING 563 FT MONMOUTH NJ 07703		Total: 33 (31 HCs, 1 CD, 1 ELECT)
1	US ARMY INFO SYS ENGRG CMND ATTN AMSEL IE TD A RIVERA FT HUACHUCA AZ 85613-5300		

INTENTIONALLY LEFT BLANK.